

Depth Descent Synchronization in $\text{SO}(D)$

Tyler Maunu · Gilad Lerman

Abstract We give robust recovery results for synchronization on the rotation group, $\text{SO}(D)$. In particular, we consider an adversarial corruption setting, where a limited percentage of the observations are arbitrarily corrupted. We give a novel algorithm that exploits Tukey depth in the tangent space, which exactly recovers the underlying rotations up to an outlier percentage of $1/(D(D-1)+2)$. This corresponds to an outlier fraction of $1/4$ for $\text{SO}(2)$ and $1/8$ for $\text{SO}(3)$. In the case of $D=2$, we demonstrate that a variant of this algorithm converges linearly to the ground truth rotations. We finish by discussing this result in relation to a simpler nonconvex energy minimization framework based on least absolute deviations, which exhibits spurious fixed points.

Keywords Robust synchronization · Structure from motion · Nonconvex optimization · Multiple rotation averaging

1 Introduction

The typical synchronization problem involves recovery of n group elements from pairwise measurements between them. It arises, for example, when solving the Structure from Motion (SfM) problem. One subproblem of SfM is to recover the three-dimensional orientations and positions of cameras from pairwise orientations and positions in relation to a scene [Özyeşil et al., 2017]. Here, we specifically focus on robust synchronization over $\text{SO}(D)$, the rotation group for \mathbb{R}^D . That is, given pairwise rotations in $\text{SO}(D)$, some of which are corrupted, we aim to recover the original set of n rotations.

We assume n unknown, ground truth elements of $\text{SO}(D)$, which we denote by $\mathbf{R}_1^*, \dots, \mathbf{R}_n^*$. We form a graph $G([n], E)$, where $[n] := \{1, \dots, n\}$ indexes the n unknown elements and E designates the edges for which measurements of relative rotations are taken. For each $jk \in E$, we are provided with the measurement

$$\mathbf{R}_{jk}^* = \mathbf{R}_j^* \mathbf{R}_k^{*\top}. \quad (1)$$

We can think of \mathbf{R}_{jk}^* in the following way: If we are oriented in the coordinate system with respect to node k , then \mathbf{R}_{jk}^* rotates our coordinate system into the coordinate system we would see if we were sitting at node j . This synchronization formulation extends to any given group, where one wishes to recover $\{g_i\}_{i=1}^n$, a subset of the group, given measurements of the group ratios $\{g_i g_j^{-1}\}_{i,j=1}^n$.

Tyler Maunu
Department of Mathematics, Massachusetts Institute of Technology
E-mail: maunut@mit.edu

Gilad Lerman
School of Mathematics, University of Minnesota
E-mail: lerman@umn.edu

In reality, we cannot hope to exactly measure the pairwise rotations in (1). In many real systems, noise and corrupted measurements frequently occur: our focus here is on corrupted measurements. Within the measurement graph G , the corruption model is assumed to be fully adversarial, which is specified by:

- We observe corrupted (or “bad”) edges $E_b \subset E$, where all edges in E_b have a corresponding arbitrary corruption. The adversary is allowed to choose E_b (and thus may to some degree influence the connectivity of $E \setminus E_b$) as well as the corrupted values \mathbf{R}_{jk} for $jk \in E_b$. For each node, the adversary is only allowed to corrupt a limited fraction of edges.
- The rest of the observed edges are uncorrupted (or “good”) edges $E_g = E \setminus E_b$, where each edge in E_g has an associated measurement given by (1).

Theoretically guaranteed methods for robust synchronization are still lacking, especially in adversarial and nonconvex settings. The development of these methods is very important because in practice measurements are usually quite corrupted, especially in applied problems like structure from motion [Özyeşil et al., 2017]. The results we establish here are concerned with *exact recovery*. That is, given a set of corrupted measurements, we wish to exactly recover $\mathbf{R}_1^*, \dots, \mathbf{R}_n^*$. We will show that this is possible for a nonconvex method even in the presence of a significant amount of arbitrary corruption.

Our method falls into the class of *multiple rotation averaging algorithms* [Govindu, 2004, Martinec and Pajdla, 2007, Hartley et al., 2013]. These methods are implementations of coordinate descent, which are a highly efficient way to solve the nonconvex program. While their analysis is challenging, it is imperative to develop a theoretical understanding of these methods and their robust counterparts [Hartley et al., 2011, Chatterjee and Govindu, 2017]. Moreover, as we discuss later, there are few robustness guarantees for group synchronization with adversarial corruption. Among the limited guarantees, none cover our model, and we thus make a significant contribution to this area. This work is also of general appeal to the nonconvex optimization community since we are able to prove convergence results in the complex nonconvex landscape of robust multiple rotation averaging. Furthermore, some energy landscapes associated with this problem exhibit many local minima and spurious fixed points, which we are able to avoid with our new method.

1.1 Contributions of This Work

The main contributions of this work follow.

1. We develop a new algorithm that we call *Depth Descent Synchronization (DDS)*. Under a generic condition on the measurement graph G , which we call the “well-connectedness”, and proper initialization, the DDS algorithm exactly recovers an underlying signal in the presence of a significant amount of adversarial outliers. This result is given in Theorem 4 and is the first guarantee of robustness to adversarial corruption for a multiple rotation averaging algorithm.
2. We show that this algorithm can be efficiently implemented in the case of $D = 2$ and $D = 3$. In particular, for $D = 2$, we give a linearly convergent algorithm which is a special case of the DDS algorithm. Its theoretical guarantees are given in Theorem 5.
3. We discuss issues arising for a common multiple rotation averaging algorithm. In particular, we demonstrate a “poorly-tempered landscape” in general, where multiple rotation averaging schemes based on the least absolute deviations energy may fail in the presence of some adversarial outliers.

While we carefully review related work later in Section 2, we emphasize here our contributions in terms of the most relevant works. Some of the only published robustness results for $\text{SO}(D)$ synchronization are in Wang and Singer [2013]. However, the probabilistic model in this work is very restrictive (see details in Section 2) and the proposed method is slow for large n .

The only existing results for adversarial robust synchronization were recently given by Lerman and Shi [2019]. Here, we briefly highlight the differences between these works.

Lerman and Shi [2019] propose a general method for group synchronization that is guaranteed to be robust to adversarial corruption. However, their method uses information from 3-cycles, that is, triangles in the graph, and so it is less efficient than typical multiple rotation averaging schemes by an order of n (the ratio

between the number of triangles and the number of edges in the graph). Beyond this, multiple rotation averaging algorithms are also attractive because they are more memory efficient. A caveat to our current work is that, while the previous discussion applies to most multiple rotation averaging algorithms, our new method is not as efficient. In particular, we require the computation of a depth-based estimator, and so each rotation update has complexity $O(n^3)$ for $\text{SO}(3)$. Therefore, we do not claim to have the most computationally efficient method for adversarially robust synchronization in terms of time complexity. However, our depth descent method does still have the benefit of more efficient memory complexity than Lerman and Shi [2019]. Beyond computational efficiency, the theoretical guarantees are also different: we bound the ratio of corrupted edges, whereas Lerman and Shi [2019] bound the ratio of corrupted triangles. The final difference from Lerman and Shi [2019] is that we require a well-connectedness condition of the graph G . Somewhat similar conditions appear, sometimes implicitly, in works minimizing energy functions [Wang and Singer, 2013, Hand et al., 2018, Lerman et al., 2018, Huang et al., 2017].

At last, we mention that the absolute deviation energy function over $\text{SO}(D)^n$ that we discuss later is similar to the one of Maunu et al. [2019] over the Grassmannian for the different problem of robust subspace recovery (RSR) [Lerman and Maunu, 2018]. However, the latter energy is “well-tempered” under a generic condition, which implies a recovery guarantee for an adversarial setting [Maunu and Lerman, 2019]. On the other hand, there are significant issues that arise in trying to prove such well-tempered results in a synchronization framework. In this work, we point out some possible difficulties that arise in establishing a well-tempered landscape for the absolute deviation energy over $\text{SO}(D)^n$, and therefore we resort to our novel robust procedure to avoid local minima. Although there are theoretical issues in proving convergence for the least absolute deviations methods, it is hard to find real examples where they actually converge to spurious minima. This fact points to some deeper phenomenon at play in practical settings that merits further theoretical study.

1.2 Notation

Bold uppercase letters will be used to denote matrices, while bold lowercase letters will be used to denote vectors. For a set \mathcal{X} in a Hilbert space, the convex hull is denoted by $\text{conv}(\mathcal{X})$. For a convex set \mathcal{X} in a Hilbert space, the relative interior is denoted by $\text{relint}(\mathcal{X})$. The sphere in \mathbb{R}^D is written as S^{D-1} . For an ordered tuple of n rotations, $\mathbf{R}_1, \dots, \mathbf{R}_n \in \text{SO}(D)$, we write $(\mathbf{R}) = (\mathbf{R}_1, \dots, \mathbf{R}_n)$.

1.3 Structure of the Rest of the Paper

We now outline the structure of this paper. First, we review related work in Section 2. Following this, in Section 3 we develop our novel Depth Descent Synchronization algorithm, which modifies the multiple rotation averaging procedure with a robust gradient estimate. Coupled with this we develop its theoretical guarantees of robustness and convergence. We then discuss the specific case of synchronization over $\text{SO}(2)$ in Section 4. Section 5 shows theoretical hurdles arising in analysis of the least absolute deviations multiple rotation averaging algorithm, and we finish in Section 6 with some open directions.

2 Related Work

Interest in the synchronization problem has grown in recent years due to applications in computer vision and image processing, such as SfM [Govindu, 2004, Martinec and Pajdla, 2007, Arie-Nachimson et al., 2012, Hartley et al., 2013, Tron and Vidal, 2009, Ozysesil et al., 2015, Boumal, 2016], cryo-electron microscopy [Wang and Singer, 2013] and Simultaneous Localization And Mapping (SLAM) [Rosen et al., 2019].

The most common formulation for solving rotation and other group synchronization problems involve a non-convex least squares formulation that can be addressed by spectral methods [Singer, 2011] or semidefinite relaxation [Bandeira et al., 2017]. On the other hand, the work of Wang and Singer [2013] uses a semidefinite relaxation of a least absolute deviations formulation to obtain a robust estimate for $\text{SO}(d)$ synchronization. They prove recovery for the pure optimizer of this convex problem in a restricted setting. In this setting the full graph is complete, every edge is corrupted with a certain probability p (in the case of $\text{SO}(2)$, they require that $p \leq 0.543$ and for $\text{SO}(3)$ they require $p \leq 0.5088$) and the corrupted group ratios are distributed uniformly on $\text{SO}(D)$. In practice, they advocate using an alternating direction augmented Lagrangian to solve their optimization problem. One may also use methods like the Burer-Monteiro formulation [Boumal et al., 2018], although current guarantees require the rank of the semidefinite program to be at least $O(\sqrt{n})$, which results in storing iterates much larger than the underlying signal that is a vector of size n [Waldspurger and Waters, 2018]. Another recent work tries to leverage a low-rank plus sparse decomposition for robust synchronization [Arrigoni et al., 2018]. However, this work does not contain robustness guarantees.

For a survey of robust rotation synchronization, see Tron et al. [2016]. Some early works on rotation synchronization include Govindu [2001, 2006], Martinec and Pajdla [2007], with later follow-up works by Hartley et al. [2013], Chatterjee and Madhav Govindu [2013], Chatterjee and Govindu [2017]. The later works discuss some least absolute deviations based approaches to multiple rotation averaging which we will discuss later. For theoretical foundations on averaging rotations, one can consult Moakher [2002]. For foundational work on optimization on the manifold $\text{SO}(d)$, see [Taylor and Kriegman, 1994, Arora, 2009].

Robust multiple rotation averaging algorithms were studied in Hartley et al. [2011] and Hartley et al. [2013]. There, the authors used a least absolute deviations formulation over $\text{SO}(3)$ using successive averaging with a Weiszfeld algorithm and a gradient-based algorithm. The authors also give a counterexample that shows that local minima exist and thus the global minimum of their problem may be hard to find in general. However, the authors give no guarantee of convergence or recovery in any setting.

A different work that does contain guarantees is that of Lerman and Shi [2019], which considers a message-passing procedure that incorporates consistent information from cycles. This algorithm was guaranteed to be robust for the adversarial setting and applies to any compact group. Although its adversarial setting is very general, it requires a bound on the ratio of corrupted cycles per edge and not on the ratio of corrupted edges. Furthermore, the use of cycles results in a more computationally intensive algorithm than the one in this work that only uses pairwise information.

In contrast to corrupted settings, some works have considered estimation in a noisy setting. Bandeira et al. [2017] study maximum likelihood estimation of the angular synchronization problem and show that the associated semidefinite relaxation is tight. More recently, message-passing algorithms have been used for maximum likelihood estimation in the Gaussian setting [Perry et al., 2018]. Other recent results leverage multiple phases to obtain better results in noisy settings [Gao and Zhao, 2019]. Minimax estimation under the squared loss over $\text{SO}(2)$ is considered in Gao and Zhang [2020], and optimization methods for the squared error over subgroups over the orthogonal group are considered in Liu et al. [2020].

Guarantees for exact recovery with adversarial, or partially adversarial, corruption appear in few other synchronization problems. The adversarial corruption in \mathbb{Z}_2 synchronization is very special since there is a single choice to corrupt a group ratio. Under a special probabilistic model, Bandeira [2018] established asymptotic and probabilistic exact recovery for the SDP relaxation of the least squares energy function of \mathbb{Z}_2 synchronization. The model assumes that $G([n], E)$ is an Erdős-Rényi graph with probability p of connection, edges are randomly corrupted with probability q and $p(1 - 2q)^2 \leq 0.5$. Huang et al. [2017] analyzed a solution for regularized least absolute deviations formulation for one-dimensional translation synchronization. Their generic condition is rather complicated and in order to interpret it they assume that $G([n], E)$ is complete. They also restrict the maximal degree of the random graph $G([n], E_b)$. Nevertheless, their interpretive model is not adversarial, but noisy. Hand et al. [2018] and Lerman et al. [2018] established asymptotic exact recovery under a probabilistic model for solutions of the different problem of location recovery from pairwise orientations. In this problem ratios of the Euclidean group are normalized to the sphere. They assume an i.i.d. Gaussian generative probabilistic model for the ground truth locations and an Erdős-Rényi model for

the graph $G([n], E)$ and further bounded the ratio of maximal degree of $G([n], E_b)$ over n . In both works, these bounds approach zero as n approaches infinity, unlike the constant bound of this work.

Another related problem over $SO(2)$ is the synchronization of Kuramoto oscillators. In particular, a primary question is the minimal graph connectivity requirement ensuring that the energy landscape is nice. The weakest known requirement is that every vertex is connected to at least $0.7889n$ other vertices [Lu and Steinerberger, 2019]. The conjectured bound is $0.75n$, which is reminiscent of the bound we require for local recovery with adversarial corruption over $SO(2)$.

Our work also fits in with the growing body of work analyzing nonconvex energy landscapes and procedures [Dauphin et al., 2014, Hardt, 2014, Jain et al., 2014, Netrapalli et al., 2014, Yi et al., 2016, Zhang and Yang, 2018, Ge et al., 2015, Lee et al., 2016, Arora et al., 2015, Mei et al., 2018, Ge et al., 2016, Boumal, 2016, Sun et al., 2015b,a, Lerman and Maunu, 2017, Cherapanamjeri et al., 2017, Ma et al., 2018, Maunu et al., 2019].

Finally, we appeal to tangent space depth, that is, using Tukey depth [Tukey, 1974] in the tangent space of the manifold $SO(D)$, to create a provable robust method. Tangent space depth, for a general manifold, first appeared in Mizera [2002], where the author proves existence and depth bounds for maximum tangent depth estimators. Earlier work on Tukey, or halfspace, depth includes Rado [1946], which proves a depth lower bound for general measures, and Danzer et al. [1963], which discusses the relation to Helly’s Theorem. More recently, the classical reference of Donoho and Gasko [1992] proves bounds on the maximum depth achieved in a dataset under ellipticity conditions. Computation of depth contours was considered in Liu [2017], Hammer et al. [2020]. Recently, an interesting connection between depth estimators and generative adversarial networks has been exhibited [Gao et al., 2018], which may perhaps lead to more computationally efficient estimators.

3 Robust Synchronization over $SO(D)$

This section considers a novel algorithm for robust synchronization over the rotation group, $SO(D)$. We assume a fixed observation graph G that encodes which pairwise rotations we observe. The pairwise rotations are written as $\mathbf{R}_{jk} \in SO(D)$, where the good edges $jk \in E_g$ have the associated observation $\mathbf{R}_j^* \mathbf{R}_k^{*\top}$, and the bad edges are arbitrarily chosen and have arbitrarily corrupted measurements.

To proceed, we must make clear our goal for the synchronization problem. In rotation synchronization there is a well known ambiguity – we can only recover \mathbf{R}^* up to right multiplication by an element of $SO(D)$. This is because, after this multiplication, one arrives at the same pairwise measurements in (1). This is a form of rotational symmetry in the nonconvex problem, which may be leveraged to develop tractable nonconvex programs [Zhang et al., 2020]. Exactly recovering the ground truth measurements $(\mathbf{R}^*) = (\mathbf{R}_1^*, \dots, \mathbf{R}_n^*) \in SO(D)^n$ up to right multiplication by $\mathbf{S} \in SO(D)$ is equivalent to finding a set of rotations $(\mathbf{R}) = (\mathbf{R}_1, \dots, \mathbf{R}_n)$ such that

$$\mathbf{R}_1^{*\top} \mathbf{R}_1 = \dots = \mathbf{R}_n^{*\top} \mathbf{R}_n = \mathbf{S}, \quad (2)$$

for some $\mathbf{S} \in SO(D)$. We refer to the set of rotations $\mathbf{R}_j^{*\top} \mathbf{R}_j, j = 1, \dots, n$, as *normalization products* since, when $(\mathbf{R}) = (\mathbf{R}^* \mathbf{S})$, they reveal the normalization factor that multiplies each element of (\mathbf{R}^*) from the right. One could extend this discussion to the case of approximate recovery by requiring that the normalization products are approximately equal.

We begin in Section 3.1 by discussing the geometry of the manifold $SO(D)$ and presenting some basic geometric results that will be used in our main theorem. Then, in Section 3.2, we outline some notions of robustness for the synchronization problem, as well as our main assumptions. Following this, Section 3.3 reviews the concept of halfspace depth from robust statistics, which will be the core tool that we use to construct our algorithm. In Section 3.4, we give our algorithm as well as its theoretical guarantees, which constitute the main innovations of this work. We finish in Section 3.5 with a discussion of how one might practically implement this algorithm.

3.1 The Manifold Structure of $SO(D)$

The rotation synchronization problem is obviously a robust recovery problem on the product Riemannian manifold $SO(D)^n$. Therefore, in the following, we freely use concepts from Riemannian geometry, and specifically those concepts related to the geometry of $SO(D)$.

The set of rotations $SO(D)$ is a $D(D-1)/2$ -dimensional Lie group that has a natural Riemannian structure. The bi-invariant distance metric $d : SO(D) \times SO(D) \rightarrow [0, \lfloor \frac{D}{2} \rfloor \pi]$ is given by

$$d(\mathbf{R}_1, \mathbf{R}_2) = \|\log(\mathbf{R}_1 \mathbf{R}_2^\top)\|_F, \quad (3)$$

where \log is the matrix logarithm. The corresponding Lie algebra is $\mathfrak{so}(D)$, the set of $D \times D$ skew-symmetric matrices. The tangent space of $SO(D)$ at $\mathbf{R} \in SO(D)$ is

$$T_{\mathbf{R}} SO(D) = \{\Delta_s \in \mathbb{R}^{d \times d} : \mathbf{R}^\top \Delta_s \in \mathfrak{so}(D)\}.$$

Notice that every tangent vector $v \in T_{\mathbf{R}} SO(D)$ has a corresponding element of $\mathfrak{so}(D)$, which we denote by $v_{\mathfrak{so}(D)}$. The corresponding Riemannian metric (which is an inner product and thus should not be confused with a distance metric) for $v, w \in T_{\mathbf{R}} SO(D)$ is given by $\langle v, w \rangle_{\mathbf{R}} = \text{Tr}(v^\top w)/2 = \text{Tr}(v_{\mathfrak{so}(D)}^\top w_{\mathfrak{so}(D)})/2$. Equipped with this metric, $SO(D)$ is a Riemannian manifold with nonnegative sectional curvature. An open ball with respect to the metric d is written as $B(\mathbf{R}, r)$, where the radius is r and the center is \mathbf{R} . Its closure and boundary are $\overline{B(\mathbf{R}, r)}$ and $\partial B(\mathbf{R}, r)$, respectively.

The exponential map is given by

$$\text{Exp}_{\mathbf{R}} : T_{\mathbf{R}} SO(D) \rightarrow SO(D), \quad \text{Exp}_{\mathbf{R}}(\mathbf{U}) = \mathbf{R} \exp(\mathbf{R}^\top \mathbf{U}), \quad (4)$$

where \exp is the matrix exponential. The logarithmic map is the inverse of this:

$$\text{Log}_{\mathbf{R}} : SO(D) \rightarrow T_{\mathbf{R}} SO(D), \quad \text{Log}_{\mathbf{R}}(\mathbf{S}) = \mathbf{R} \log(\mathbf{R}^\top \mathbf{S}). \quad (5)$$

The geodesic between $\mathbf{R}, \mathbf{S} \in SO(D)$ is written as $\overrightarrow{\mathbf{R}\mathbf{S}}(t) = \text{Exp}_{\mathbf{R}}(t \text{Log}_{\mathbf{R}}(\mathbf{S}))$, for $t \in [0, 1]$. In the following, we use the notation for a halfspace of $T_{\mathbf{R}} SO(D)$,

$$\mathcal{H}(\mathbf{R}, v) = \{u \in T_{\mathbf{R}} SO(D) : \langle u, v \rangle_{\mathbf{R}} > 0, \text{Exp}_{\mathbf{R}}(tu) \text{ is a geodesic for } t \in [0, 1]\}. \quad (6)$$

The following result is standard in the literature [Karcher, 1977, Afsari, 2009, Petersen, 2016].

Theorem 1 *In a closed ball $\overline{B(\mathbf{C}, r)} \subset SO(D)$ with $r < \pi/2$, the squared distance metric d^2 is strictly convex. This implies, in particular, that for all $\mathbf{R}_0, \mathbf{R}_1 \in \overline{B(\mathbf{C}, r)}$, $\overrightarrow{\mathbf{R}_0 \mathbf{R}_1}(t) \in B(\mathbf{C}, r)$ for all $t \in (0, 1)$.*

Note that the closed ball in the previous theorem has the property that the interior of any nonconstant geodesic lies strictly in the interior of the ball. The following result is also readily apparent. It states that, for boundary points on a sufficiently small ball in $SO(D)$, all interior directions are contained in a halfspace.

Corollary 1 *Let \overline{B} be a ball on $SO(D)$ with radius $r < \pi/2$ and $\mathbf{R} \in \partial B$. Then, there is a halfspace $\mathcal{H} \subset T_{\mathbf{R}} SO(D)$ such that $\text{Log}_{\mathbf{R}} \overline{B} \subset \mathcal{H}$.*

The final lemma of this section states that if a discrete set of rotations \mathcal{R} is contained in a ball, and if half of the ball contains no boundary measurements, then the set \mathcal{R} is actually contained in a ball of smaller radius.

Lemma 1 *Let $B = B(\mathbf{C}, r) \subset SO(D)$ and $\mathcal{R} \subset \overline{B}$ a finite set of rotations. Suppose that there exists $v \in T_{\mathbf{C}} SO(D)$ such that*

$$\text{Exp}_{\mathbf{C}}[\overline{\mathcal{H}(\mathbf{C}, -v)}] \cap \partial B \cap \mathcal{R} = \emptyset.$$

Then, \mathcal{R} is contained in a ball with radius less than r .

Proof Let $c(t)$ be the geodesic $\text{Exp}_{\mathcal{C}}(tv)$. We claim that, for t sufficiently small, $\mathcal{R} \subset B(c(t), r)$, which is an open ball. Heuristically, one should expect this to be true, since the closed halfspace $\overline{\mathcal{H}(\mathcal{C}, -v)}$ contains no boundary points, and so moving the center a small amount in the v direction keeps all points within the ball.

By the first order approximation to $d^2(c(t), \mathbf{R})$ and since $\angle(v, \text{Log}_{\mathcal{C}} \mathbf{R}) < \pi/2$, we have

$$d(c(t), \mathbf{R})^2 < d(c(0), \mathbf{R})^2, \quad \forall \mathbf{R} \in \mathcal{R} \cap \text{Exp}_{\mathcal{C}}(\overline{\mathcal{H}(\mathcal{C}, v)}), \quad (7)$$

for t sufficiently small. On the other hand, since

$$\text{Exp}_{\mathcal{C}}[\overline{\mathcal{H}(\mathcal{C}, -v)}] \cap \partial B \cap \mathcal{R} \subset B(\mathcal{C}, r),$$

the distance to \mathcal{C} over all $\mathbf{R} \in \text{Exp}_{\mathcal{C}}[\overline{\mathcal{H}(\mathcal{C}, -v)}] \cap \partial B \cap \mathcal{R}$ is bounded away from r . By continuity of $d(c(t), \mathbf{S})$ for all $\mathbf{R} \in \mathcal{R}$, this implies that there is an ϵ such that

$$d(c(t), \mathbf{R}) < r, \quad \forall t \in (0, \epsilon). \quad (8)$$

Putting (7) and (8) together implies that a small shift of the ball results in a new center such that $\max_{\mathbf{R} \in \mathcal{R}} d(c(t), \mathbf{R}) < r$. In turn, this means that all points of \mathcal{R} lie in a ball $\overline{B}(c(t), r')$ with $r' < r$. \square

3.2 Notions of Robustness

In order to quantify our notion of robustness, we introduce the following terminology. Recall that we have an underlying graph $G([n], E)$ corresponding to the pairwise measurements, where E is partitioned into an inlier set, E_g , and outlier set E_b . For any $j \in [n]$, we define the its neighborhood as well as the inlier and outlier neighborhoods as

$$E^j = E_g^j \cup E_b^j, \quad E_g^j := \{k \in [n] : jk \in E_g\}, \quad E_b^j := \{k \in [n] : jk \in E_b\}. \quad (9)$$

We will denote by α_0 the maximum percentage of outliers per node. That is, α_0 is the maximum of $\#(E_b^j)/n_j$ over all $j \in [n]$, where throughout the rest of the paper $\#(\cdot)$ denotes the number of points in a set and n_j is the degree of node j , $n_j = \#(E^j)$.

The following notion of recovery threshold is related to the notion of a breakdown point in robust statistics. However, our goal is somewhat different, since we desire an exact estimator rather than an approximation, as is typically considered for classical breakdown points. This is similar to the notion of RSR breakdown point given in Section 1.1 of Maunu and Lerman [2019].

Definition 1 (Recovery Threshold) The recovery threshold of a robust rotation synchronization algorithm is the largest value of α_0 such that the algorithm outputs an estimator $(\hat{\mathbf{R}})$ that satisfies (2).

The simplest information-theoretic bound for the recovery threshold is $\alpha_0 \leq 1/2$. Indeed, if $\alpha_0 > 1/2$, then an adversary could easily choose E_b to have a subgraph that dominates E_g with a consistent set of measurements for an alternative signal $(\mathbf{R}^b) = (\mathbf{R}_1^b, \dots, \mathbf{R}_n^b)$. That is, the observations would be

$$\mathbf{R}_{jk} = \begin{cases} \mathbf{R}_j^{*\top} \mathbf{R}_k^*, & jk \in E_g \\ \mathbf{R}_j^{b\top} \mathbf{R}_k^b, & jk \in E_b. \end{cases} \quad (10)$$

If the adversary chooses the partition E_g and E_b properly, then one could easily think that \mathbf{R}^b is the true underlying signal.

For many nonconvex methods, good initialization is quite important [Li et al., 2019, Maunu et al., 2019, Qu et al., 2019, Chi et al., 2019, Qu et al., 2020]. As we will see in the theory we develop, we only obtain recovery after initializing in a neighborhood of \mathbf{R}^* . For reference, we state the initialization assumption here.

Definition 2 A set of n rotations (\mathbf{R}) lies within a ρ -neighborhood of (\mathbf{R}^*) if the normalization products $\mathbf{R}_j^{*\top} \mathbf{R}_j$ all lie in a ball of radius ρ . That is, there exists a $\mathbf{C} \in \text{SO}(D)$ such that

$$d(\mathbf{C}, \mathbf{R}_j^{*\top} \mathbf{R}_j) < \rho, \forall j = 1, \dots, n.$$

With this terminology, we state our main assumption on the initialization.

Assumption 2 The initial set of rotations $(\mathbf{R}(0))$ for our algorithm lies within a $\pi/2$ -neighborhood of (\mathbf{R}^*) .

As we discuss in Section 3.5, we believe that this assumption is not so restrictive, and we later give some intuition for how this might occur in a real scenario.

Finally, while corruptions are arbitrary, we require an assumption on the underlying graph G . The main assumption on this graph is a well-connectedness condition that we define in the following.

Assumption 3 (Well-connectedness condition) For $J \subset [n]$ such that $\#(J) \leq n/2$, there exists an index $j \in J$ such that

$$\# [E^j \cap ([n] \setminus J)] > \# [E^j \cap J]. \quad (11)$$

In other words, the node j is connected to more nodes outside of J than inside of J .

We believe that this assumption is nontrivial, and we give some examples of simple graphs satisfying this condition in Figure 1. This condition bears some similarity to the notions of conductance and graph expansion, and further examination of this condition and its connections to these other notions of connectedness in graph theory is left to future work.

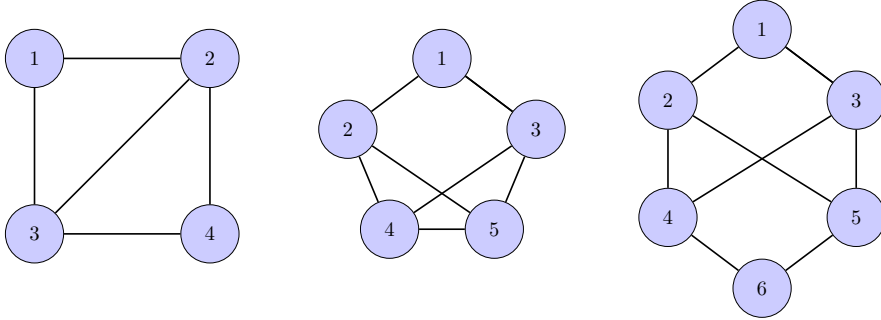


Fig. 1 Examples of graphs that satisfy the well-connectedness condition for $n = 4, 5$ and 6 . In each of these graphs, (11) is satisfied: that is, all subsets J of size at most $n/2$, there exists a node $j \in J$ such that $\#(E^j \cap ([n] \setminus J)) > \#(E^j \cap J)$.

3.3 Tukey Depth and its Properties

We will use the concept of *Tukey depth* to determine descent directions on the manifold $\text{SO}(D)^n$, although other notions of depth could potentially be used as well (see Ch. 58 of Toth et al. [2017] for a discussion of different notions of depth). In Euclidean space, the Tukey depth of a point $\mathbf{x} \in \mathbb{R}^D$ in a dataset $\mathcal{X} = \{\mathbf{x}_1, \dots, \mathbf{x}_n\} \subset \mathbb{R}^D$ is given by

$$\text{depth}(\mathbf{x}, \mathcal{X}) = \min_{\mathbf{u} \in S^{D-1}} \#\{\mathbf{x}_i \in \mathcal{X} : \mathbf{u}^\top (\mathbf{x}_i - \mathbf{x}) \geq 0\} \quad (12)$$

The depth is therefore the minimum number of points contained in any halfspace that has \mathbf{x} in its separating hyperplane. A natural robust estimator is then the point of maximum depth, which is also called the Tukey median. The β -depth level set for $\beta \in [0, 1]$ is defined by

$$\mathcal{D}_\beta(\mathcal{X}) = \{\mathbf{y} \in \mathbb{R}^D : \text{depth}(\mathbf{y}, \mathcal{X}) \geq \beta \#(\mathcal{X})\}. \quad (13)$$

This level set is convex and compact, and its boundary is made up of hyperplanes defined by sets of D points [Liu et al., 2019]. This function will be used in the construction of our algorithm.

We recall the following theorem, which bounds the maximum possible depth within a general dataset. Notice that, in particular, this guarantees that the depth level set $\mathcal{D}_\beta(\mathcal{X})$ is nonempty for all $\beta \leq 1/(D+1)$.

Proposition 1 (Rado [1946]) *Suppose that \mathcal{X} is a set of n points. Then, the maximum depth in \mathcal{X} is bounded below by $\lceil n/(D+1) \rceil$.*

A particularly useful property of Tukey depth is that it is *affine equivariant*, that is, it is stable under affine transformations.

Lemma 2 (Donoho and Gasko [1992])

$$\text{depth}(\mathbf{A}\mathbf{x} + \mathbf{b}, \mathbf{A}\mathcal{X} + \mathbf{b}) = \text{depth}(\mathbf{x}, \mathcal{X}).$$

This implies, in particular, that things behave nicely if we change the inner product on \mathbb{R}^D .

$$\begin{aligned} \min_{\mathbf{u} \in S^{D-1}} \#\{\mathbf{x}_i \in \mathcal{X} : \mathbf{u}^\top \mathbf{A}(\mathbf{x}_i - \mathbf{x}) \geq 0\} &= \text{depth}(\mathbf{A}\mathbf{x}, \mathbf{A}\mathcal{X}) \\ &= \text{depth}(\mathbf{x}, \mathcal{X}). \end{aligned} \quad (14)$$

With this property, we can map between the depth regions in $(\mathbb{R}^D, \langle \cdot, \cdot \rangle)$ and $(\mathbb{R}^D, \langle \cdot, \mathbf{A} \cdot \rangle)$ by

$$\mathbf{A}\mathcal{D}_\beta(\mathcal{X}) = \mathcal{D}_\beta(\mathbf{A}\mathcal{X}). \quad (15)$$

This affine equivariance implies, in particular, that Proposition 1 extends to datasets in $T_{\mathbf{R}}\text{SO}(D)$.

We finish with a simple lemma on depth level sets that will be the key to the robustness guarantee for our later algorithm. For a halfspace $H(\mathbf{0}, \mathbf{v}) := \{\mathbf{x} \in \mathbb{R}^D : \mathbf{v}^\top \mathbf{x} \geq 0\} \subset \mathbb{R}^D$, we write its separating hyperplane as $L(\mathbf{0}, \mathbf{v})$.

Lemma 3 *Suppose that we have a dataset $\mathcal{X} = \{\mathbf{x}_1, \dots, \mathbf{x}_n\} \in \mathbb{R}^D$ and a subset $\mathcal{Y} \subset \mathcal{X}$ that satisfies the properties i) $\#\mathcal{Y} > n - n/(2D+2)$, ii) There exists closed halfspace $\overline{H(\mathbf{0}, \mathbf{v})} \subset \mathbb{R}^D$ such that $\overline{H(\mathbf{0}, \mathbf{v})} \supset \mathcal{Y}$, and iii) $\mathcal{Y} \cap L(\mathbf{0}, \mathbf{v}) = \{\mathbf{0}\}$ or \emptyset . Then, $\text{relint}(\mathcal{D}_{1/(2D+2)}(\mathcal{X})) \subset \text{conv}(\mathcal{Y}) \subset (H(\mathbf{0}, \mathbf{v}) \cup \{\mathbf{0}\})$. Beyond this, if $\#\mathcal{Y} \cap L(\mathbf{0}, \mathbf{v}) < n/2$, then $\text{relint}(\mathcal{D}_{1/(2D+2)}(\mathcal{X})) \subset H(\mathbf{0}, \mathbf{v})$.*

Proof It is obvious by the properties of depth that $\text{relint}(\mathcal{D}_{1/(2D+2)}(\mathcal{X})) \subset \text{conv}(\mathcal{Y}) \subset (H(\mathbf{0}, \mathbf{v}) \cup \{\mathbf{0}\})$, since any point on the boundary of $\text{conv}(\mathcal{Y})$ has depth less than $1/(2D+2)$. By Proposition 1, there is a point of depth at least $1/(2D+2)$, and so $\mathcal{D}_{1/(2D+2)}(\mathcal{X})$ is nonempty.

Suppose that less than $n/2$ points in \mathcal{Y} are zero, that is, $\#\mathcal{Y} \cap L(\mathbf{0}, \mathbf{v}) < n/2$. We claim that $\mathcal{D}_{1/(2D+2)}(\mathcal{X}) \cap H(\mathbf{0}, \mathbf{v}) \neq \emptyset$. Define the auxiliary set $\mathcal{Z} = \mathcal{X} \setminus (\mathcal{Y} \cap L(\mathbf{0}, \mathbf{v}))$, that is, \mathcal{Z} removes the $\mathbf{0}$ values in \mathcal{Y} from \mathcal{X} . Since $\#\mathcal{Y} \cap L(\mathbf{0}, \mathbf{v}) < n/2$, we have that $m = \#\mathcal{Z} \geq n/2$. Within \mathcal{Z} , there is a point $\hat{\mathbf{z}}$ of depth at least $m/(D+1)$. Further, since $n \leq 2m$ and $\#\mathcal{X} \cap H(\mathbf{0}, -\mathbf{v}) < n/(2D+2)$, we have

$$\#\mathcal{X} \cap H(\mathbf{0}, \mathbf{v}) > m - \frac{n}{2D+2} = m \frac{D}{D+1},$$

which implies that $\hat{\mathbf{z}}$ must lie in $H(\mathbf{0}, \mathbf{v})$. On the other hand, since $m \geq n/2$, we have that

$$\text{depth}(\hat{\mathbf{z}}, \mathcal{X}) \geq \frac{m}{D+1} \geq \frac{n}{2(D+1)},$$

which means that $\hat{\mathbf{z}}$ is a point of depth at least $1/(2D+2)$ in \mathcal{X} . □

3.4 Depth Descent Synchronization

We now use the results of the previous section to derive an algorithm. We assume a *selection rule* $\mathcal{S}_{\mathbf{R}}$ on convex, compact subsets of $T_{\mathbf{R}}\text{SO}(D)$ for all $\mathbf{R} \in \text{SO}(D)$ that selects a point. In particular, for our theorem, we assume that this selection rule chooses a point in the relative interior, although another selection rule that works in our theory is to select the furthest point from $\mathbf{0}$. To select a point in the relative interior, one selection rule could be to take a point uniformly at random, or another could be to take the center of mass. As our theorem makes clear, the choice of this selection rule does not affect the exact recovery result, but it may change convergence rates. Since we do not give quantitative convergence rates in this work, we leave this choice as arbitrary until we discuss the specific case of $\text{SO}(2)$ in Section 4.

In any case, given a selection rule $\mathcal{S}_{\mathbf{R}}$ over such subsets of $T_{\mathbf{R}}\text{SO}(d)$, suppose our estimated rotations at time t are $(\mathbf{R}(t))$. Our update direction at this time for index $j = t \bmod n$ is defined by

$$v_j(t) = \mathcal{S}_{\mathbf{R}}(\mathcal{D}_{\beta}(\{\text{Log}_{\mathbf{R}_j(t)} \mathbf{R}_{jk} \mathbf{R}_k(t) : k \in E^j\})). \quad (16)$$

Then, given $v_j(t)$, the algorithm updates

$$j = t \bmod n, \mathbf{R}_j(t+1) = \text{Exp}_{\mathbf{R}_j(t)}(\eta(t)v_j(t)), \mathbf{R}_k(t+1) = \mathbf{R}_k(t) \text{ for } k \in [n] \setminus \{j\}. \quad (17)$$

for a chosen step size $\eta(t) \in (0, \eta^*(D)]$. Our theory below restricts this step size according to Theorem 4.2 of Afsari et al. [2013]: in the case of $D = 2$ or 3 , one can take $\eta^*(D) = 1$, while for $D > 3$ the upper bound is more restrictive (the reader can consult the discussion in Afsari et al. [2013] for a more thorough discussion of the bound). For sake of clarity, we write the full DDS algorithm in Algorithm 1.

Algorithm 1 Depth Descent Synchronization for $\text{SO}(D)$

Require: $\mathbf{R}(0)$, number of iterations T , selection rule \mathcal{S} , $\eta \in (0, \eta^*(D)]$ step size, β depth parameter
for $t = 1, \dots, T$ **do**
 $j = t \bmod n$
 $v_j(t) = \mathcal{S}_{\mathbf{R}}(\mathcal{D}_{\beta}(\{\text{Log}_{\mathbf{R}_j(t)} \mathbf{R}_{jk} \mathbf{R}_k(t) : k \in E^j\}))$
 $\mathbf{R}_j(t+1) \leftarrow \text{Exp}_{\mathbf{R}_j(t)}(\eta v_j(t))$
 $\mathbf{R}_k(t+1) \leftarrow \mathbf{R}_k(t), k \neq j$
end for
return $\mathbf{R}(T)$

The following theorem constitutes the main theoretical result of this work. It states that, with proper initialization and well-connectedness, the recovery threshold of Algorithm 1 is $1/(D(D-1)+2)$.

Theorem 4 *Suppose that $\alpha_0 < 1/(D(D-1)+2)$, Assumptions 2 and 3 hold, and $[(\mathbf{R}(t))]_{t \in \mathbb{N}}$ is generated by (17) with $\beta = 1/(D(D-1)+2)$. Further assume in the case of $D = 2, 3$ that $\eta \in (0, 1]$, and in the case of $D > 3$ that η is chosen according to Theorem 4.2 of Afsari et al. [2013]. Then, $d(\mathbf{R}_j^{*\top} \mathbf{R}_j(t), \mathbf{R}_k^{*\top} \mathbf{R}_k(t)) \rightarrow 0$ for all j, k , and the DDS algorithm exactly recovers (\mathbf{R}^*) .*

As examples, in the case of $\text{SO}(2)$, Theorem 4 yields a corruption threshold of $\alpha_0 < 1/4$. In the case of $\text{SO}(3)$, Theorem 4 yields a corruption level of $\alpha_0 < 1/8$.

To aid in the proof, we denote the smallest ball enclosing our normalization products as

$$B(t) := \text{argmin}_{B(\mathbf{C}, \rho)} \rho, \text{ s.t. } \mathbf{R}_1^{*\top} \mathbf{R}_1(t), \dots, \mathbf{R}_n^{*\top} \mathbf{R}_n(t) \in \overline{B(\mathbf{C}, \rho)}. \quad (18)$$

The center of $B(t)$ is $\mathbf{C}(t)$ and its radius is $r(B(t))$. Our goal will be to show that $r(B(t)) \rightarrow 0, t \rightarrow \infty$.

Proof (Proof of Theorem 4)

The proof of the theorem is broken into three parts. In the first part, we prove that the sequence $[(\mathbf{R}(t))]_{t \in \mathbb{N}}$ remains in a nested sequence of balls. In the second part, we show that, after sufficiently many iterations,

the radius of the smallest enclosing ball must shrink. We finish in the third part by appealing to a general convergence theorem for monotonic algorithms.

Part I: $B(t+1) \subseteq \overline{B(t)}$: First, we show that at time t , no matter which index is updated, the normalization products remain in $\overline{B(t)}$. This is true at $t = 0$, so assume that it is true at a time t . Let $j = t \bmod n$ and consider the pairwise measurements in the tangent space at $\mathbf{R}_j(t)$: for each $k \in E_g^j$, the corresponding point in the tangent space is given by $\text{Log}_{\mathbf{R}_j(t)}(\mathbf{R}_j^* \mathbf{R}_k^{\star\top} \mathbf{R}_k(t))$. By assumption, we have that $\mathbf{R}_j^* \mathbf{R}_k^{\star\top} \mathbf{R}_k(t) \in \mathbf{R}_j^* \overline{B(t)}$ for all k . Since $\alpha_0 < 1/(D(D-1)+2)$ and $\beta = 1/(D(D-1)+2)$,

$$\mathcal{D}_{1/(2D+2)}(\{\text{Log}_{\mathbf{R}_j(t)}(\mathbf{R}_{jk} \mathbf{R}_k(t)) : k \in E^j\}) \subset \text{conv}(\{\text{Log}_{\mathbf{R}_j(t)}(\mathbf{R}_{jk} \mathbf{R}_k(t)) : k \in E_g^j\}),$$

since the set in the right-hand side of the display contains more than a $1 - \beta$ fraction of points. We can now apply Theorem 3.7 of Afsari et al. [2013]. This follows from the fact that the update direction $v_j(t)$ is the gradient of the Fréchet mean function for a weighted combination of $\{\text{Log}_{\mathbf{R}_j(t)}(\mathbf{R}_{jk} \mathbf{R}_k(t)) : k \in E_g^j\}$ (since it lies in the convex hull of these points). More formally, letting $m = \#(E_g^j)$, since $v_j(t) \in \text{conv}(\{\text{Log}_{\mathbf{R}_j(t)}(\mathbf{R}_{jk} \mathbf{R}_k(t)) : k \in E_g^j\})$, there exist weights a_1, \dots, a_m such that

$$\begin{aligned} v_j(t) &= \sum_{i=1}^m a_i \text{Log}_{\mathbf{R}_j(t)} \mathbf{R}_{jk_i} \mathbf{R}_{k_i}(t) \\ &= \sum_{i=1}^m a_i \text{Log}_{\mathbf{R}_j(t)} \mathbf{R}_j^* \mathbf{R}_{k_i}^{\star\top} \mathbf{R}_{k_i}(t) \\ &= -\text{grad} \sum_{i=1}^m a_i d^2(\mathbf{R}_{k_i}^{\star\top} \mathbf{R}_{k_i}(t), \cdot) \Big|_{\mathbf{R}_j(t)}. \end{aligned}$$

Therefore, choosing the step size as in Afsari et al. [2013] implies that $\mathbf{R}_j^{\star\top} \mathbf{R}_j(t+1) \in \overline{B(t)}$, and further that $\mathbf{R}_j^{\star\top} \mathbf{R}_j(t+1) \in B(t)$ when $v_j(t) \neq 0$. In turn, this implies that $\overline{B(t+1)} \subseteq \overline{B(t)}$ and, if $\mathbf{R}_j(t) \in B(t)$, then $\mathbf{R}_j(t+1) \in B(t)$ as well (i.e., interior points cannot move to the boundary).

In the case of $\text{SO}(3)$, Theorem 3.7 of Afsari et al. [2013] tells us that choosing $\eta \in (0, 1]$ suffices. The case of $\text{SO}(D)$ for $D > 3$ is dealt with in a similar way using Theorem 4.2 of Afsari et al. [2013].

Part II: $r(B(s + \Delta_s)) < r(B(s))$: We now must show that after sufficiently many iterations, the radius of $B(t)$ strictly decreases. To this end, fix a time s . At this time, at least one normalization product $\mathbf{R}_j^{\star\top} \mathbf{R}_j(s)$ must lie on the boundary $\partial B(s)$. For convenience, define the index set $J(s)$ of boundary rotations at time s by

$$J(s) := \left\{ j : \mathbf{R}_j^{\star\top} \mathbf{R}_j(s) \in \partial B(s) \right\}.$$

We will show that there exists a $\Delta_s > 0$ such that at some future time $s + \Delta_s$,

$$r(B(s + \Delta_s)) < r(B(s)). \quad (19)$$

To this end, pick a direction w uniformly at random from $T_{C(s)} \text{SO}(D)$ such that $\|w\|_{C(s)} = 1$. This vector separates $T_{C(s)}$ into two halfspaces, and thus partitions $B(s)$ into two halves. One of these halves contains at most $n/2$ points $\text{Log}_{C(s)}(\mathbf{R}_j^{\star\top} \mathbf{R}_j(s))$, and we will denote the corresponding halfspace of $T_{C(s)} \text{SO}(D)$ by \mathcal{H} . Since the direction w is chosen uniformly at random, there are no points on the boundary of this halfspace with probability 1.

Let $K(s)$ denote the set

$$K(s) := \{k : \mathbf{R}_k^{\star\top} \mathbf{R}_k(s) \in \text{Exp}_{C(s)}(\mathcal{H}) \cap \partial B(s)\},$$

that is, the set of indices corresponding to boundary normalization products at time s . At each time $t = s + m$ for $m > 0$, if none of the normalization products $\mathbf{R}_k^{\star\top} \mathbf{R}_k(t)$, $k \in K(s)$, lie in $\partial B(s)$, then set $\Delta_s = m$ and we can apply Lemma 1 to yield (19).

Otherwise, by Assumption 3, there is at least one index $k \in K(s)$ such that $\mathbf{R}_k^{*\top} \mathbf{R}_k(s)$ is in $\partial B(s)$ and

$$\#(E^k \setminus K(s)) > \#(E^k \cap K(s)).$$

Suppose that we update this index k at time $t = s + m$. We are in a situation where we can apply Lemma 3, with

$$\mathcal{X} = \{\text{Log}_{\mathbf{R}_j(t)} \mathbf{R}_{jk} \mathbf{R}_k(t) : k \in E^j\}, \quad \mathcal{Y} = \{\text{Log}_{\mathbf{R}_j(t)} \mathbf{R}_{jk} \mathbf{R}_k(t) : k \in E_g^j\},$$

which yields that $v_j(s+m) \in \text{conv}(\mathcal{Y})$ and $v_j(s+m) \neq 0$. Thus, for sufficiently small $\eta(s+m)$, $\mathbf{R}_j(s+m+1) \in B(s)$. Repeating this sequentially for all elements of $K(s)$, there must exist a Δ_s such that

$$\mathbf{R}_j^{*\top} \mathbf{R}_j(s + \Delta_s) \in B(s), \quad \forall j \in K(s).$$

We are left in a situation where $\mathbf{R}_1^{*\top} \mathbf{R}_1(s + \Delta_s), \dots, \mathbf{R}_n^{*\top} \mathbf{R}_n(s + \Delta_s) \in \overline{B(s)}$, and there exists a w such that $\mathcal{H}(C(s), -w)$ contains no boundary points. By appealing to Lemma 1, we know that $(\mathbf{R}(s + \Delta_s))$ lies in a ball of radius smaller than $r(B(s))$, and therefore $r(B(s))$ has a strictly monotonic subsequence.

Part III: Strict monotonicity implies convergence: By Mizera [2002], as long as $\beta \leq 1/(D(D-1)/2+1)$, the point to set mapping

$$\mathbf{R}_j(t) \mapsto D_\beta(\{\log_{\mathbf{R}_j(t)}(\mathbf{R}_{jk} \mathbf{R}_k(t)) : k \in E^j\})$$

is non-empty and outer semicontinuous with respect to the empirical measure on

$$\{\text{Log}_{\mathbf{R}_j(t)} \mathbf{R}_{jk} \mathbf{R}_k(t) : k \in E^j\}.$$

Therefore, the associated algorithm (17) is upper semicontinuous in the sense of Theorem 3.1 of Meyer [1976], and we obtain convergence of $\mathbf{R}(t)$ to a fixed point of (17).

We finish by examining fixed points of the algorithm (17). Suppose that \mathbf{R} is a fixed point of this sequence, such that v_j as defined by (16) is zero. Examining the application of Lemma 3 above, we see that this only happens if, for all j , $d(\mathbf{R}_j, \mathbf{R}_j^* \mathbf{R}_k^{*\top} \mathbf{R}_k) = 0$ for at least $n_j/2$ measurements k . Together with the well-connectedness condition of Assumption 3, this implies that $d(\mathbf{R}_j, \mathbf{R}_j^* \mathbf{R}_k^{*\top} \mathbf{R}_j) = 0$ for all j, k . \square

3.5 Implementation

While this paper is primarily focused on the theory of robust rotation synchronization, we still believe that it is valuable to discuss the practical implementation of this algorithm. Future work will go into implementing and testing this method for real datasets, to both verify robustness to adversarial outliers as well as test real-world accuracy.

At least in low-dimensions, depth regions can be calculated efficiently for small datasets [Liu et al., 2019]. In particular, the most straightforward algorithm involves an exhaustive search over hyperplanes spanned by D -subsets of \mathcal{X} that cut off βn points in \mathcal{X} . The time complexity of this method for \mathbb{R}^3 is $O(n^3 \log(n))$, and so could be used for moderately sized datasets. Translating this to our problem in $\text{SO}(3)$, the time complexity for updating $j \in [n]$ is $O(n_j^3 \log(n_j))$, and so we see that this method is efficient for sparser graphs. On the other hand, in an Erdős-Rényi model, the complexity to update all n rotations is $O(n^4 p^3)$, where p is the Erdős-Rényi parameter.

As discussed in the introduction, the time complexity of the DDS algorithm is not necessarily more efficient than that of Lerman and Shi [2019]. Indeed, the complexity of their message-passing algorithm is $O(n^3)$ for a single update to all rotations, while for our method it is $O(\sum_j n_j^3 \log(n_j))$. On the other hand, our complexity is better in $\text{SO}(2)$, where depth contours can be easily found in $O(n \log(n))$ by sorting, and it thus takes $O(n^2 \log(n))$ time to update all nodes. Finally, we also note that our method has better scaling in terms of memory usage: the multiple rotation averaging scheme takes $O(n)$ memory while the message-passing scheme takes $O(n^3)$.

Another benefit of our method current method is that there is no need to tune the step size, which is due to the local convexity properties of the manifold. As we outlined in our main theorem, the step size can be directly selected from the guidance of Afsari et al. [2013]. One detail that is left to future work is to examine the effect of the selection rule, both in terms of its effect on computational efficiency and convergence rate.

Finally, Assumption 2 requires that we initialize the DDS algorithm so that the normalization products lie in sufficiently small ball. This can be achieved in practice for cameras whose orientations lie close enough together. That is, suppose that all of the rotations $\mathbf{R}_1^{\star\top}, \dots, \mathbf{R}_n^{\star\top}$ lie in $B(\mathbf{S}, \rho)$ for all j , for some \mathbf{S} and $\rho < \pi/2$. Then, if the the initial point for the DDS algorithm is chosen to be $(\mathbf{I}, \dots, \mathbf{I})$, then it is not hard to see that

$$\mathbf{R}_j^{\star\top} \mathbf{I} = \mathbf{R}_j^{\star\top} \in B(\mathbf{S}, \rho), \quad \forall j \in [n]. \quad (20)$$

which directly shows that Assumption 2 holds. A weakening of this initialization condition, for example by only requiring that neighbors lie in neighborhoods of each other, is left to future work.

4 An Illustration in $\text{SO}(2)$

To further illustrate the DDS method, we consider the case of synchronization over $\text{SO}(2)$, where the method becomes considerably simpler due to the 1-dimensional manifold structure. First, Section 4.1 gives definitions of some geometrical objects on $\text{SO}(2)$, which we identify with \mathbb{C}_1 for mathematical convenience. Then, in Section 4.2, we choose a particular selection rule for the DDS algorithm and to define our $\text{SO}(2)$ synchronization method. Finally, Section 4.3 gives the adversarial recovery and convergence guarantee under the assumption of well-connected measurement graphs.

4.1 The Geometry of \mathbb{C}_1

We define a few structures related to the manifold \mathbb{C}_1 . The tangent space can be identified with \mathbb{R} . Let $v \in T_z \mathbb{C}_1$ be a unit direction in the tangent space at z_j (i.e., $v = \pm 1$). The geodesic originating at z_j in the direction v is given by $\gamma(t) = e^{ivt} z_j$, $t \in [0, \pi/|v|]$. The exponential map and inverse exponential map (logarithm map) on this 1-dimensional manifold are given by

$$\text{Exp}_z(\theta) = e^{i\theta} z, \theta \in (-\pi, \pi], \quad \text{Log}_z(y) = \arg(y\bar{z}). \quad (21)$$

Finally, the *cut-locus* of a point $z \in \mathbb{C}_1$ is defined as the set of points for which there is not a unique geodesic from z . It is not hard to see that this is given by $\text{cut}(z) = \{-z\}$.

Recall that we seek an underlying signal $\mathbf{z}^* \in \mathbb{C}_1^n$. Notice that its elements, $z_j^* \in \mathbb{C}_1$ for $j \in [n]$, can be parameterized by angles, $z_j^* = e^{i\theta_j^*}$. This angle is also known as the argument of the complex number, and so we write $\arg(e^{i\theta}) = \theta$, where $\theta \in (-\pi, \pi]$. The angular, or geodesic, distance between z_1 and $z_2 \in \mathbb{C}_1$ is

$$d_{\mathcal{L}}(z_1, z_2) = |\arg(z_1 \bar{z}_2)|. \quad (22)$$

For later reference, we plot the extended angular distance function in Figure 2.

Recall that if $jk \in E_g$, then the edge measurement is correct, that is, $z_{jk} = z_{jk}^*$, where $z_{jk}^* := z_j^* \bar{z}_k^*$ is defined analogously to (1). For $jk \in E_b$, the measurement z_{jk} is assumed to be an arbitrary element of \mathbb{C}_1 . Within the measurements z_{jk}^* , $jk \in E_g$, \mathbf{z}^* is only identified up to a global rotation, due to the rotational ambiguity discussed in Section 3. To deal with this ambiguity, the following function will be used to demonstrate convergence of a sequence to \mathbf{z}^* :

$$\delta(\mathbf{z}) = \max_{jk \in E} d_{\mathcal{L}}(z_{jk}^* \bar{z}_j, \bar{z}_k z_{jk}) \quad (23)$$

This is again nothing but a function that measures the maximum distance between normalization products. Notice that $\delta(\mathbf{z}) = 0 \iff \mathbf{z} = \mathbf{z}^* \cdot y$ for some rotation $y \in \mathbb{C}_1$. Therefore, convergence of $\delta(\mathbf{z})$ to zero indicates convergence of \mathbf{z} to \mathbf{z}^* , and an algorithm exactly recovers \mathbf{z}^* iff $\delta(\mathbf{z}) \rightarrow 0$. Finally, we note that in the case of $\text{SO}(2)$, Assumption 2 becomes the requirement that $\delta(\mathbf{z}(0)) < \pi$.

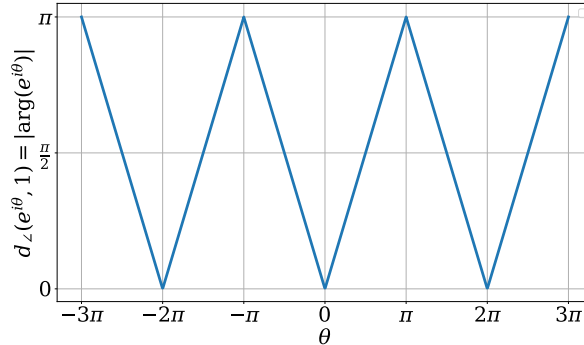


Fig. 2 The angular distance function $d_{\perp}(e^{i\theta}, 1)$.

4.2 Trimmed Averaging Synchronization

For a 1-dimensional dataset $\mathcal{X} = \{x_i\}$, the formulation of depth is quite simple:

$$\text{depth}(x, \mathcal{X}) = \min(\#\{x_i \leq x\}, \#\{x_i \geq x\}). \quad (24)$$

With this in mind, the β -depth level set is

$$D_{\beta}(\mathcal{X}) = [x_{(\lceil \beta n \rceil)}, x_{(\lfloor (1-\beta)n \rfloor)}], \quad (25)$$

where $x_{(i)}$ denotes the i th order statistic. Therefore, to specify the DDS algorithm, it remains to specify a selection rule. One selection rule that could be used with the framework of Section 3 is to select the average of all points that fall within the trimmed range interval (25), which results in a trimmed averaging procedure. We call this specific algorithm for $\text{SO}(2)$ the Trimmed Averaging Synchronization (TAS) algorithm. An illustration of one trimmed averaging step is given in Figure 3. The interior region of (25) is the interval between the empirical β and $(1 - \beta)$ quantiles. For a discrete $\mathcal{X} \subset \mathbb{R}$ and a fraction $0 < p < 1$, we write the p th quantile of \mathcal{X} by \mathcal{X}_p . It is convenient to define the trimming operator

$$\mathcal{T}_{0.25}\mathcal{X} = \mathcal{X} \cap D_{0.25}(\mathcal{X}) = \{x \in \mathcal{X} : \mathcal{X}_{0.25} \leq x \leq \mathcal{X}_{0.75}\}. \quad (26)$$

We also denote the average of a dataset $\mathcal{X} \subset \mathbb{R}$ by $\text{ave}(\mathcal{X})$. That is, $\text{ave}(\mathcal{X}) = (\sum_{x \in \mathcal{X}} x) / \#(\mathcal{X})$.

Due to the simplified geometry of $\text{SO}(2)$, we will show in the following that using this trimmed rotation averaging scheme converges to the underlying solution linearly when the percentage of outliers is at most $\alpha_0 < 1/4$ when G is fully connected. In the case where G is not fully connected, the result is a corollary of Theorem 4 under the assumption of well-connectedness. We note that this fraction is similar to the one given in Lerman and Shi [2019], although there the bound is formulated for corrupted triangles in the graph. Beyond exact recovery, trimmed means are also appealing due to the fact that they are more efficient than the median for Cauchy noise distributions [Bloch, 1966], although it is unclear if such results translate to \mathbb{C}_1 .

As before, the indices j are updated in a cyclic fashion. We give the TAS algorithm in Algorithm 2. To allow for damping of the updates, we include the step-size parameter $\eta \in (0, 1]$. When $\eta < 1$, we refer to the algorithm as η -Damped TAS or η -DTAS for short.

4.3 Recovery Guarantees for DTAS

The following theorem gives the main recovery result for the η -DTAS algorithm. While the algorithm converges linearly, the rate we derive depends on n and is worst-case. In the few simulations we have run, the

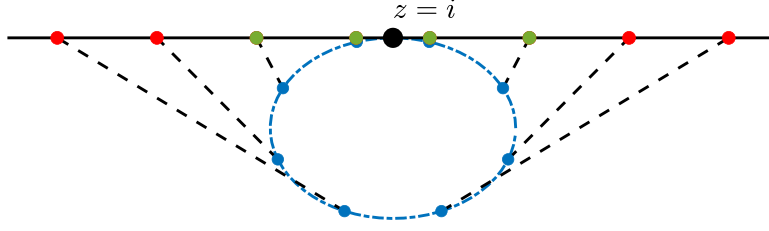


Fig. 3 Illustration of the TAS algorithm at a fixed step and a fixed node j . The measurement is $z_j = z = i$. After projecting into the tangent space, the outermost points in red are filtered, and the green points are averaged.

Algorithm 2 η -Damped Trimmed Averaging Synchronization

Require: $z(0)$, number of iterations T , damping parameter $\eta \in (0, 1]$

for $t = 1, \dots, T$ **do**

$j = t \bmod n$

$z_j(t+1) \leftarrow \text{Exp}_{z_j(t+1)} \left[\eta \cdot \text{ave} \left(\mathcal{T}_{0.25} \left\{ \text{Log}_{z_j(t+1)} (z_{jk} z_k(t)) : k \in E^j \right\} \right) \right]$

$z_k(t+1) \leftarrow z_k(t), k \neq j$

end for

return $z(T)$

algorithm seems to converge at a faster rate that merits more study. Also, a more complicated proof may yield linear convergence in the general case of well-connected G , but for sake of brevity, we only prove it for the fully connected case.

Theorem 5 *Suppose that $\alpha_0 < 1/4$, Assumption 2 holds, G satisfies Assumption 3, and $[z(t)]_{t \in \mathbb{N}}$ is the sequence generated by η -DTAS, for $\eta \in (0, 1)$. Then, $\delta(z(t)) \rightarrow 0$, and the algorithm exactly recovers z^* . Further, in the case where G is fully connected, the DTAS algorithm linearly converges to z^* .*

Proof The proof of convergence under well-connectedness follows from the fact that, when updating index j at iteration t , the selection rule defined by choosing the trimmed average yields a point in the relative interior of $D_{1/4}(\{\text{Log}_{z_j(t)}(z_{jk} z_k(t)) : k \in E^j\})$.

To see linear convergence in the fully connected case, we prove that all normalization products $\overline{z_j^*} z_j(t)$ contract during each pass over the dataset. Denote

$$\delta_j = \theta_j(t) - \theta_j^* \in [-\delta(z(t))/2, \delta(z(t))/2]. \quad (27)$$

These are the translation of the normalization products to the angular coordinates of the points $z_1(t), \dots, z_n(t)$. Also, define the sets

$$I_+(t) = \{k : \arg(\overline{z_j^*} z_j(t)) > 0\}, \quad I_-(t) = \{k : \arg(\overline{z_j^*} z_j(t)) \leq 0\}. \quad (28)$$

In this proof, we will write $\delta = \delta(z(t))$ as a shorthand. Notice that we must have

$$\min(\#I_+(t), I_-(t)) \leq n/2,$$

unless $I_+(t) = I_-(t) = [n]$, in which case $z(t) = z^* w$ for some $w \in \mathbb{C}_1$ and $z(t)$ recovers z^* .

For the update with respect to index j , all good pairwise measurements must lie in $-\delta_j + [-\delta/2, \delta/2]$. Since there are at least $3n_j/4$ good measurements, all trimmed points must lie in this interval as well. Therefore, for all $j \in I_-(t)$, after updating we have

$$\overline{z_j^*} z_j(t) \in \exp [i[-\delta/2, \eta\delta/2]]. \quad (29)$$

Using this fact, we will now show that the indices in $I_+(t)$ must move inwards. Indeed, since $\#I_+(t) \leq n/2$, we must have $\#(E_g^j \cap I_-(t)) \geq 1$ for all $j \in I_+(t)$. Therefore, for each trimmed mean for $j \in I_+(t)$, we have

$$\begin{aligned} \text{ave} \left(\mathcal{T}_{0.25} \left(\left\{ \text{Log}_{z_j(t)}(z_{jk}z_k(t)) : k \neq j \right\} \right) \right) &\leq \frac{2}{n-1} \left[\eta \frac{\delta}{2} - \delta_j + \left(\frac{n-1}{2} - 1 \right) \left(\frac{\delta}{2} - \delta_j \right) \right] \\ &\leq \left(\frac{n-3}{n-1} - \frac{2}{n-1} \eta \right) \cdot \frac{\delta}{2} - \delta_j. \end{aligned} \quad (30)$$

Thus,

$$\begin{aligned} \eta \text{ave} \left(\mathcal{T}_{0.25} \left(\left\{ \text{Log}_{z_j(t)}(z_{jk}z_k(t)) : k \in E^j \right\} \right) \right) + \delta_j &\leq \eta \left(\frac{n-3-2\eta}{n-1} \right) \cdot \frac{\delta}{2} + (1-\eta)\delta_j \\ &\leq \eta \left(\frac{n-3}{n-1} \right) \cdot \frac{\delta}{2} + (1-\eta)\frac{\delta}{2} \\ &= \frac{\delta}{2} \left(1 - \eta \left[\frac{2}{n-1} \right] \right). \end{aligned} \quad (31)$$

After the coordinate update, we have that for all $j \in I_+(t)$,

$$\overline{z_j^*} z_j(t) \in \exp \left(i \left[-\frac{\delta}{2}, \left(1 - \eta \left(\frac{2}{n-1} \right) \frac{\delta}{2} \right) \right] \right). \quad (32)$$

After repeating this argument for all j over the course of the epoch, this yields that

$$\overline{z_j^*} z_j(t+1) \in \exp \left(i \left[-\frac{\delta}{2}, \left(1 - \eta \left(\frac{2}{n-1} \right) \frac{\delta}{2} \right) \right] \right),$$

as long as $\eta < (n-1)/(n+1)$. The width of this interval is $(n-1-\eta)\delta(z(t))/(n-1)$, which yields the desired result. \square

5 L_1 Multiple Rotation Averaging

We demonstrate the strength of our theory by comparing to another popular nonconvex algorithm for robust synchronization. In particular, we discuss robust multiple rotation averaging that utilizes an L_1 energy [Dai et al., 2009, Hartley et al., 2011, Chatterjee and Govindu, 2017]. Outside of a result for a convex relaxation and a specific probabilistic model of data [Wang and Singer, 2013], past works on this method offer no guarantees of robustness, although they show strong empirical performance. Many L_1 Multiple Rotation Averaging algorithms (L_1 -MRA) boil down to doing coordinate descent, while others use IRLS on individual coordinates [Hartley et al., 2011] or on the whole set of coordinates [Chatterjee and Govindu, 2017]. These previous cases also primarily focused on optimization over $\text{SO}(3)$.

To highlight theoretical issues arising in the analysis of these methods, we consider optimization over $\text{SO}(2)$, since the theoretical analysis is simpler. We note, however, that the issues that arise directly extend to $\text{SO}(D)$ since one can embed $\text{SO}(2)$ within the higher-dimensional manifold. Further, $\text{SO}(2)$ is the easiest case for our previous depth based algorithm, and so one could hope that L_1 -MRA may have a simpler analysis as well. Our hope is that this discussion will spur future work on this topic.

In this section, we review the existing approaches to synchronization based on the least absolute deviations energy. First, Section 5.1 reviews the L_1 energy minimization problem proposed for synchronization over $\text{SO}(2)$. After this, in Section 5.2 we discuss a simple variant of L_1 -MRA that uses coordinate descent. We finish in Section 5.3 by discussing some issues arising in the analysis of this algorithm.

5.1 Robust Synchronization by Energy Minimization

Dai et al. [2009], Hartley et al. [2011], Wang and Singer [2013] and Chatterjee and Govindu [2017] consider the following least absolute deviations formulation

$$\min_{\mathbf{z} \in \mathbb{C}_1^n} F_{\angle}(\mathbf{z}) := \sum_{j < k} d_{\angle}(z_j, z_{jk}z_k). \quad (33)$$

In the same way that the median is a robust estimator of the center of a dataset, the least absolute deviations estimator is expected to give a robust estimate of the underlying set of rotations in synchronization.

It is helpful to define the coordinate energy function

$$F_{\angle}^j(y; \mathbf{z}) = \sum_{k \in [n] \setminus j} d_{\angle}(y, z_{jk}z_k). \quad (34)$$

To analyze robustness properties of local minimizers of this energy, we can calculate directional derivatives of F_{\angle}^j . Notice that the energy (33) minimizes the deviations between z_j and “estimates” of z_j given by $z_{jk}z_k$, for $k \in [n] \setminus j$. For a given $\mathbf{z} = (z_1, \dots, z_n)$ and $j \in [n]$, we break up the set of these estimates into parts:

$$C_+(j; \mathbf{z}) := \left\{ y = z_{jk}z_k : \text{Log}_{z_j}(y) \in (0, \pi), k \in [n] \setminus j \right\}, \quad (35)$$

$$C_-(j; \mathbf{z}) := \left\{ y = z_{jk}z_k : \text{Log}_{z_j}(y) \in (-\pi, 0), k \in [n] \setminus j \right\}, \quad (36)$$

$$C_0(j; \mathbf{z}) := \left\{ y = z_{jk}z_k = z_j \right\}, \quad (37)$$

$$\text{cut}(j; \mathbf{z}) := \left\{ y = z_{jk}z_k = -z_j \right\}. \quad (38)$$

In geometric terms, the set $C_+(j; \mathbf{z})$ represents all estimates $z_{jk}z_k$ such that they have positive value in the tangent space at z_j , and similarly the set $C_-(j; \mathbf{z})$ have negative value in the tangent space at z_j . The set $C_0(j; \mathbf{z})$ represent estimates $z_{jk}z_k$ that exactly equal z_j , while the set $\text{cut}(j; \mathbf{z})$ represents points that lie at the cut-locus with respect to z_j .

Let $v \in T_{z_j} \mathbb{C}_1$ be a unit direction and $\gamma(t) = e^{ivt}z_j$ a geodesic in \mathbb{C}_1 . It is not hard to convince oneself that the directional derivative of $F_{\angle}^j(\cdot; \mathbf{z})$ at z_j is given by

$$\begin{aligned} \partial_v F_{\angle}^j(z_j; \mathbf{z}) &= \left. \frac{d}{dt} F_{\angle}^j(\gamma(t); \mathbf{z}) \right|_{t=0} = \lim_{h \rightarrow 0} \frac{F_{\angle}^j(\gamma(h); \mathbf{z}) - F_{\angle}^j(\gamma(0); \mathbf{z})}{h} \\ &= \lim_{h \rightarrow 0} \frac{\sum_{k \in [n] \setminus j} d_{\angle}(e^{ihvt}z_j, z_{jk}z_k) - \sum_{k \in [n] \setminus j} d_{\angle}(z_j, z_{jk}z_k)}{h} \\ &= \text{sign}(v)(-\#C_+(j; \mathbf{z}) + \#C_-(j; \mathbf{z})) - \#\text{cut}(j; \mathbf{z}). \end{aligned} \quad (39)$$

This follows from the fact that the energy is really just a sum of absolute angular distances.

5.2 Variants of the L_1 -MRA Algorithm

We present a variant of coordinate descent-based L_1 -MRA [Dai et al., 2009, Hartley et al., 2011]. At time t , one updates the index $j = t \bmod n$. Of course, this is just for ease of analysis, and one could consider other strategies, such as randomly sampling j for every update.

To update index j , we make most improvement in minimizing (33) by attempting to solve $z_j(t) \in \text{argmin}_{z \in \mathbb{C}_1} F_{\angle}^j(z; \mathbf{z}(t))$. One can accomplish this by searching for a local minimum of $F_{\angle}^j(z; \mathbf{z}(t))$ after initializing at $z_j(t)$, which is done using a line-search in a direction of decrease from $z_j(t)$. This direction can be found by choosing $v = \pm 1$ such that $\partial_v F_{\angle}^j(z_j; \mathbf{z}) < 0$.

Along the geodesic given by $e^{ivt}z_j$, the directional derivatives $\partial_v F_{\angle}^j(e^{ivt}z_j; \mathbf{z})$ are constant until $e^{ivt}z_j = \pm z_{jk}z_k$, for some $k \in [n]$. In this case, the value of $\partial_v F_{\angle}^j(e^{ivt}z_j; \mathbf{z})$ either increases or decreases by $\#\{k : e^{ivt}z_j = \pm z_{jk}z_k\}$. Therefore, the algorithm searches in the direction v until the first point $e^{ivt}z_j$ is found such that

$$e^{ivt}z_j \in \left\{ \pm z_{jk}z_k : k \in [n] \right\}, \quad \partial_v F_{\angle}^j(e^{ivt}z_j; \mathbf{z}) \geq 0. \quad (40)$$

This variant of L_1 -MRA is termed Gradient Descent L_1 -MRA (GD- L_1 -MRA), and we give the full algorithm in Algorithm 3.

Algorithm 3 GD- L_1 Multiple Rotation Averaging [Dai et al., 2009, Hartley et al., 2011]

Require: $z(0)$, number of iterations T

```

for  $t = 1, \dots, T$  do
   $z(t+1) \leftarrow z(t)$ 
   $j \leftarrow t \bmod n$ 
  if  $\min_{v \in \{\pm 1\}} \partial_v F_{\angle}^j(z_j; z(t+1)) < 0$  then
     $v \leftarrow \operatorname{argmin}_{v \in \{\pm 1\}} \partial_v F_{\angle}^j(z_j; z(t+1))$ 
     $Y = \operatorname{Log}_{z_j(t)} \left( C_{\operatorname{sign}(v)}(j, z(t+1)) \cup (-C_{-\operatorname{sign}(v)}(j, z(t+1))) \right)$ 
     $Y_+ = \{y \in Y : \partial_v F_{\angle}^j(\operatorname{Exp}_{z_j(t)}(y); z(t+1)) \geq 0\}$ 
     $z_j(t+1) \leftarrow \exp_{z_j(t)} \left( \operatorname{argmin}_{y \in Y_+} |y| \right)$ 
  end if
end for
return  $z(T)$ 

```

The only fixed points for this algorithm occur when every point is a local minimum with respect to the coordinate directions. We state this as follows. If \mathbf{z} is a fixed point of the GD- L_1 -MRA algorithm, then $\partial_v F_{\angle}^j(z_j; \mathbf{z}) \geq 0$ for $v \in \{\pm 1\}$ and for all j . Therefore, each coordinate sits at its own local minimum, which is just to say that moving each coordinate alone does not decrease the cost. However, this does not preclude the existence of a geodesic in \mathbb{C}_1^n along which the full cost $F(\mathbf{z})$ decreases. This issue is discussed further in Section 5.3.

We finish by giving two simple lemmas on the properties of using GD- L_1 -MRA to solve (33). The first lemma implies, with proper initialization, the iterates of L_1 -MRA must remain in the local neighborhood $\delta(z(t)) < \pi$, as long as the ratio of bad edges per node is not too large. Notice here that there are no restrictions on the measurement graph other than it must be connected.

Lemma 4 *Suppose Assumption 2 holds, G is connected, and that $\alpha_0 < 1/2$. Then, if $\{z(t)\}_{t \in \mathbb{N}}$ is the sequence generated by GD- L_1 -MRA, $\delta(z(t+1)) \leq \delta(z(t))$.*

Proof At iteration t , we will show that the coordinate descent mapping satisfies the bounded iteration property. Suppose we are updating the j th coordinate at iteration t . Then, the updated coordinate $z_j(t+1)$ is found by running gradient descent initialized at $z_j(t)$ until a local minimum is found for the energy function $F_{\angle}^j(z; z(t))$.

The next iterate $z_j(t+1)$ minimizes a sum of absolute deviations with $z_{jk}z_k(t)$, where the inlier terms are given by $z_j^* \overline{z_k^*} z_k(t)$. Notice that, for all $jl, jk \in E_g$,

$$\begin{aligned} \max_{l, k \in E_g^j} d_{\angle}(z_{jl}z_l(t), z_{jk}z_k(t)) &= \max_{l, k \in E_g^j} d_{\angle}(z_l(t), \overline{z_{jl}} z_{jk}z_k(t)) \\ &= \max_{l, k \in E_g^j} d_{\angle}(z_l(t), z_{lk}z_k(t)) \leq \delta(\mathbf{z}(t)). \end{aligned}$$

This implies that all the points $z_{jk}^* z_k(t)$ lie within a circular interval of width less than π , which we write as $e^{i[a, b]}$. Notice that, for sufficiently small ϵ , $\partial_{+1} F_{\angle}^j(z; \mathbf{z}(t)) < 0$ for $z \in e^{i(a-\epsilon, a)}$ and $\partial_{-1} F_{\angle}^j(z; \mathbf{z}(t)) < 0$

for $z \in e^{i(b,b+\epsilon)}$ since more than $n/2$ points lie in $e^{i[a,b]}$. Therefore, the function $F_{\mathcal{L}}^j(z; z(t))$ must have at least one local minimum in $e^{i[a,b]}$ that is found by L_1 -MRA. It then follows that

$$\delta(z(t+1)) \leq \delta(z(t)). \quad (41)$$

□

The second lemma shows that GD- L_1 -MRA is strictly monotonic.

Lemma 5 *If $\{z(t)\}_{t \in \mathbb{N}}$ is the sequence generated by GD- L_1 -MRA, then the sequence of function values $\{F_{\mathcal{L}}(z(t))\}_{t \in \mathbb{N}}$ is strictly monotonic.*

Proof We can break up the energy function $F_{\mathcal{L}}$ in the following way:

$$\begin{aligned} F_{\mathcal{L}}(z) &= \sum_{j < k} d_{\mathcal{L}}(z_j, z_{jk} z_k) \\ &= \sum_{k \in [n] \setminus j} d_{\mathcal{L}}(z_j, z_{jk} z_k) + \sum_{\substack{l < k \\ l, k \in [n] \setminus j}} d_{\mathcal{L}}(z_j, z_{jk} z_k). \end{aligned} \quad (42)$$

All dependence on z_j is in the first sum. Notice that our iteration finds a local minimum for the first sum with respect to z_j , and further that it must find a local minimum that has less energy than $z_j(t)$ since the line-search procedure starts at $z_j(t)$. If $z_j(t)$ is not already a local minimum for its coordinate function, then one of the directional derivatives is strictly negative. This implies that the L_1 -MRA procedure is strictly monotonic unless $z_j(t)$ is fixed. □

These results are insufficient to give convergence of L_1 -MRA to z^* due to two issues we discuss in Section 5.3. These issues are: 1) the coordinate descent mapping defined by GD- L_1 -MRA is not necessarily closed in the adversarial setting, and 2) there may be spurious fixed points. Indeed, it has been pointed out before that the general proof of convergence for such methods is hard, as is mentioned in Section 7.4 of [Hartley et al., 2013]. These issues stand in contrast to practical scenarios where we observe convergence, and so new tools must be brought to bear in order to analyze this method.

5.3 Issues Arising in the Analysis of L_1 -MRA

We briefly present two issues that arise in the analysis of the coordinate descent mapping. To our knowledge, these issues have not yet been addressed in the robust multiple rotation averaging literature. First, we show that the mapping defined by this algorithm may not be closed. Then, we discuss spurious fixed points for the GD- L_1 -MRA procedure.

First, the coordinate mapping given by Algorithm 3 may not be closed. Suppose that we update index j at iteration t . As the following example illustrates, all issues with the map not being closed have to do with the points located at the cut locus of $z_j(t)$. This property prevents the application of Zangwill's global convergence theorem [Zangwill, 1969].

Example 1 (The map $z(t) \mapsto z(t+1)$ is not closed) As a simple example, suppose we have a signal with 6 components, and the GD- L_1 -MRA procedure is initialized at $z(0) = (1, e^{ic}, e^{ic}, e^{-ic}, -1, -1)$ for $c < \pi$, and $z_{jk} = 1$ for all $jk \in E$. Suppose further that we wish to update $z_1(0)$ at iteration 1. Then, it is obvious that $\partial_{+1} F_{\mathcal{L}}^1(1; z(0)) < 0$, since this direction moves the signal closer to the coordinates z_k for $k = 2, 3, 4, 5$. Therefore, we find that $z(1) = (e^{ic}, e^{ic}, e^{ic}, e^{-ic}, -1, -1)$. However, it is quite easy to come up with a sequence that takes steps in the opposite direction. Indeed, consider the sequence $z_l(0) = (1, e^{ic}, e^{ic}, e^{-ic}, -e^{i/l}, -e^{i/l})$ for $l \in \mathbb{N}$. We see that $z_l(0) \rightarrow z(0)$. However, updating the first coordinate of $z_l(0)$ yields $z_l(1) = (e^{-ic}, e^{ic}, e^{ic}, e^{-ic}, -e^{i/l}, -e^{i/l})$. As $l \rightarrow \infty$, $z_l(1) \not\rightarrow z^1$. Therefore, GD- L_1 -MRA mapping is not closed in general.

A second issue is the existence of spurious fixed points. These even exist in the case where G is fully connected and there is one outlier per edge.

Lemma 6 (No Outliers) *Suppose that G is a fully connected graph with n even. For each j , suppose E_b^j only contains one element. Then, there exists an adversarial corruption choice such that there are spurious fixed points \hat{z} where $0 < \delta(\hat{z}) < \pi$.*

Proof Partition $[n]$ into two sets of equal size. Call these sets J and K . Without loss of generality we can choose $J = \{1, 2, \dots, n/2\}$ and $K = \{n/2+1, \dots, n\}$. Choose \hat{z} to be such that $\hat{z}_j \overline{\hat{z}_j} = \hat{z}_{j'} \overline{\hat{z}_{j'}} = e^{i\theta}$ for all $j, j' \in J$, and $\hat{z}_k \overline{\hat{z}_k} = \hat{z}_{k'} \overline{\hat{z}_{k'}} = 1$ for all $k, k' \in K$, and such that $0 < \delta(\hat{z}) < \pi$. Without loss of generality, assume that $\theta \in (0, \pi/2)$.

As the adversary, suppose that we define the set of bad edges as

$$E_b = \{jk : j = k + n/2\},$$

so that bad edges only exist between the sets J and K . In particular, this implies that for each $j \in J$, E_g^j contains $n/2 - 1$ good edges jj' , for $j' \in J$, and $n/2 - 1$ edges jk for $k \in K$. Conversely, all $k \in K$ have $n/2 - 1$ good edges within K and $n/2 - 1$ good edges to J .

For a node $j \in J$, notice that the good pairwise measurements are $z_j^* \overline{z_k^*} z_k$. Consider the directional derivative in the -1 direction at some z_j for $j \in J$. Then, each $jk \in E_g^j$ contributes a $+1$ if $k \in J$ and -1 if $k \in K$. Therefore if for the bad edge $jk \in E_b^j$ the adversary chooses z_{jk} such that $z_{jk} z_j = e^{i(\theta+\epsilon)}$ for $\epsilon > 0$ sufficiently small, this contributes $+1$ to the directional derivative, and so the $v = -1$ direction is a direction of increase. Similarly, the $v = +1$ direction is obviously a direction of increase, since the directional derivative is $n - 2$ (in this direction, j only moves closer to the corrupted edge value). Therefore, every j is fixed. \square

In some sense, this indicates that the subgraph of good edges being too well-connected can hinder the convergence of GD- L_1 -MRA. For any point \hat{z} satisfying the implications of Lemma 6, the energy decreases along geodesic between \hat{z} and z^* . However, in order to find this decrease, we see that one must move blocks of coordinates together, which GD- L_1 -MRA cannot do. We currently do not have easy fixes for these problems. Some potential ways to deal with these issues could involve regularization, either by smoothing the energy function or by using some sort of random subsampling, but we leave such developments to future work.

6 Conclusion

In this work, we developed the first adversarial robustness guarantees for a multiple rotation averaging algorithm. Our novel algorithm relies on finding descent directions using Tukey depth in the tangent space of $\text{SO}(D)$. In the case of $D = 2$ and $D = 3$, which most frequently arise in practice, our recovery thresholds are $1/4$ and $1/8$, and the algorithm can be implemented efficiently. We also discuss some theoretical issues that arise when one tries to analyze the optimization landscape of the least absolute deviations multiple rotation averaging algorithm.

Future work should examine what the limits of this analysis are, as well as if tighter analyses can yield larger recovery thresholds. At least for the cases of $\text{SO}(2)$ and $\text{SO}(3)$, which arise in applications, the depth descent estimator discussed in this paper has significant recovery thresholds, while also being computationally tractable.

Two more concrete directions for future work would be to see if the well-connectedness condition in Assumption 3 can be relaxed at all, what its implications are, and when it actually holds. A concrete way forward might be to explore its connections with conductance and graph expansion. Another way forward would be to prove recovery results instead under other assumptions on the graph, such as conductance bounds.

While we discuss some theoretical issues arising in the analysis of the L_1 -MRA algorithm, in practice these algorithms tend to perform quite well. Therefore, these methods warrant more study, and in particular, future analysis should determine conditions under which this method is able to converge and recover a set

of underlying rotations. It may be that such methods are not stable to adversarial outliers, and so one could assume some more restrictions on the bad edges. It would be interesting to see what sorts of results are achievable in the non-adversarial setting for all of the discussed methods. As inspiration, in the problem of robust subspace recovery, one can take the percentage of corruption to 1 and still obtain exact recovery under very special models of data [Maunu et al., 2019]. It would be interesting to see if nonconvex methods for synchronization enjoy similar guarantees.

Finally, perhaps the most important direction for future work is to give theoretically justified algorithms for a larger range of algorithms employed for SfM [Özyeşil et al., 2017, Bianco et al., 2018]. Indeed, such theoretical work can lead to new and improved algorithms and also to the development of novel state-of-the-art pipelines.

References

- B. Afsari, R. Tron, and R. Vidal. On the convergence of gradient descent for finding the Riemannian center of mass. *SIAM Journal on Control and Optimization*, 51(3):2230–2260, 2013.
- Bijan Afsari. *Means and averaging on Riemannian manifolds*. PhD thesis, University of Maryland, College Park, 2009.
- M. Arie-Nachimson, S. Z. Kovalsky, I. Kemelmacher-Shlizerman, A. Singer, and R. Basri. Global motion estimation from point matches. In *2012 Second International Conference on 3D Imaging, Modeling, Processing, Visualization & Transmission*, pages 81–88. IEEE, 2012.
- R. Arora. On learning rotations. In *Advances in neural information processing systems*, pages 55–63, 2009.
- S. Arora, R. Ge, T. Ma, and A. Moitra. Simple, efficient, and neural algorithms for sparse coding. *arXiv preprint arXiv:1503.00778*, 2015.
- F. Arrigoni, B. Rossi, P. Fragneto, and A. Fusiello. Robust synchronization in $SO(3)$ and $SE(3)$ via low-rank and sparse matrix decomposition. *Computer Vision and Image Understanding*, 174:95–113, 2018.
- A. S. Bandeira, N. Boumal, and A. Singer. Tightness of the maximum likelihood semidefinite relaxation for angular synchronization. *Mathematical Programming*, 163(1-2):145–167, 2017.
- Afonso S. Bandeira. Random Laplacian matrices and convex relaxations. *Foundations of Computational Mathematics*, 18(2):345–379, 2018. doi: 10.1007/s10208-016-9341-9.
- S. Bianco, G. Ciocca, and D. Marelli. Evaluating the performance of structure from motion pipelines. *Journal of Imaging*, 4(8):98, 2018.
- D. Bloch. A note on the estimation of the location parameter of the cauchy distribution. *Journal of the American Statistical Association*, 61(315):852–855, 1966.
- N. Boumal. Nonconvex phase synchronization. *SIAM Journal on Optimization*, 26(4):2355–2377, 2016.
- N. Boumal, V. Voroninski, and A. S. Bandeira. Deterministic guarantees for Burer–Monteiro factorizations of smooth semidefinite programs. *arXiv preprint arXiv:1804.02008*, 2018.
- A. Chatterjee and V. M. Govindu. Robust relative rotation averaging. *IEEE transactions on pattern analysis and machine intelligence*, 40(4):958–972, 2017.
- A. Chatterjee and V. Madhav Govindu. Efficient and robust large-scale rotation averaging. In *Proceedings of the IEEE International Conference on Computer Vision*, pages 521–528, 2013.
- Y. Cherapanamjeri, P. Jain, and P. Netrapalli. Thresholding based outlier robust PCA. In *COLT*, pages 593–628, 2017.
- Y. Chi, Y. Lu, and Y. Chen. Nonconvex optimization meets low-rank matrix factorization: An overview. *IEEE Transactions on Signal Processing*, 67(20):5239–5269, 2019.
- Y. Dai, J. Trumpf, H. Li, N. Barnes, and R. Hartley. Rotation averaging with application to camera-rig calibration. In *Asian Conference on Computer Vision*, pages 335–346. Springer, 2009.
- L. Danzer, B. Grünbaum, and V. Klee. Helly’s theorem and its relatives. In *Proc. Symp. Pure Math.*, volume 7, pages 101–180. Amer. Math. Soc., 1963.

- Y. N. Dauphin, R. Pascanu, C. Gulcehre, K. Cho, S. Ganguli, and Y. Bengio. Identifying and attacking the saddle point problem in high-dimensional non-convex optimization. In *Advances in neural information processing systems*, pages 2933–2941, 2014.
- D. L. Donoho and M. Gasko. Breakdown properties of location estimates based on halfspace depth and projected outlyingness. *The Annals of Statistics*, 20(4):1803–1827, 1992.
- C. Gao and A. Y. Zhang. Exact minimax estimation for phase synchronization. *arXiv preprint arXiv:2010.04345*, 2020.
- C. Gao, J. Liu, Y. Yao, and W. Zhu. Robust estimation and generative adversarial nets. *arXiv preprint arXiv:1810.02030*, 2018.
- T. Gao and Z. Zhao. Multi-frequency phase synchronization. *arXiv preprint arXiv:1901.08235*, 2019.
- R. Ge, F. Huang, C. Jin, and Y. Yuan. Escaping from saddle points—online stochastic gradient for tensor decomposition. In *Proceedings of The 28th Conference on Learning Theory*, pages 797–842, 2015.
- R. Ge, J. D. Lee, and T. Ma. Matrix completion has no spurious local minimum. *arXiv preprint arXiv:1605.07272*, 2016.
- V. M. Govindu. Combining two-view constraints for motion estimation. In *Proceedings of the 2001 IEEE Computer Society Conference on Computer Vision and Pattern Recognition. CVPR 2001*, volume 2, pages II–II. IEEE, 2001.
- V. M. Govindu. Lie-algebraic averaging for globally consistent motion estimation. In *Proceedings of the 2004 IEEE Computer Society Conference on Computer Vision and Pattern Recognition, 2004. CVPR 2004.*, volume 1, pages I–I. IEEE, 2004.
- V. M. Govindu. Robustness in motion averaging. In *Asian Conference on Computer Vision*, pages 457–466. Springer, 2006.
- H. L. Hammer, A. Yazidi, and H. Rue. Estimating tukey depth using incremental quantile estimators. *arXiv preprint arXiv:2001.02393*, 2020.
- P. Hand, C. Lee, and V. Voroninski. Exact simultaneous recovery of locations and structure from known orientations and corrupted point correspondences. *Discrete & Computational Geometry*, 59(2):413–450, 2018.
- M. Hardt. Understanding alternating minimization for matrix completion. In *FOCS*, pages 651–660. IEEE, 2014.
- R. Hartley, K. Aftab, and J. Trunpf. L1 rotation averaging using the Weiszfeld algorithm. In *Computer Vision and Pattern Recognition (CVPR), 2011 IEEE Conference on*, pages 3041–3048. IEEE, 2011.
- R. Hartley, J. Trunpf, Y. Dai, and H. Li. Rotation averaging. *International journal of computer vision*, 103(3):267–305, 2013.
- X. Huang, Z. Liang, C. Bajaj, and Q. Huang. Translation synchronization via truncated least squares. In *Advances in Neural Information Processing Systems 30: Annual Conference on Neural Information Processing Systems 2017, 4-9 December 2017, Long Beach, CA, USA*, pages 1459–1468, 2017.
- P. Jain, A. Tewari, and P. Kar. On iterative hard thresholding methods for high-dimensional M-estimation. In *Advances in Neural Information Processing Systems*, pages 685–693, 2014.
- H. Karcher. Riemannian center of mass and mollifier smoothing. *Communications on pure and applied mathematics*, 30(5):509–541, 1977.
- J. D. Lee, M. Simchowitz, M. I. Jordan, and B. Recht. Gradient descent converges to minimizers. *University of California, Berkeley*, 1050:16, 2016.
- G. Lerman and T. Maunu. Fast, robust and non-convex subspace recovery. *Information and Inference: A Journal of the IMA*, 7(2):277–336, 2017.
- G. Lerman and T. Maunu. An overview of robust subspace recovery. *Proceedings of the IEEE*, 106(8): 1380–1410, 2018.
- G. Lerman and Y. Shi. Robust group synchronization via cycle-edge message passing. *arXiv preprint arXiv:1912.11347*, 2019.
- G. Lerman, Y. Shi, and T. Zhang. Exact camera location recovery by least unsquared deviations. *SIAM Journal on Imaging Sciences*, 11(4):2692–2721, 2018.

- X. Li, S. Ling, T. Strohmer, and K. Wei. Rapid, robust, and reliable blind deconvolution via nonconvex optimization. *Applied and computational harmonic analysis*, 47(3):893–934, 2019.
- H. Liu, M.-C. Yue, and A. So. A unified approach to synchronization problems over subgroups of the orthogonal group. *arXiv preprint arXiv:2009.07514*, 2020.
- X. Liu. Fast implementation of the Tukey depth. *Computational Statistics*, 32(4):1395–1410, 2017.
- X. Liu, K. Mosler, and P. Mozharovskiy. Fast computation of tukey trimmed regions and median in dimension $p > 2$. *Journal of Computational and Graphical Statistics*, 28(3):682–697, 2019.
- J. Lu and S. Steinerberger. Synchronization of Kuramoto oscillators in dense networks. *arXiv preprint arXiv:1911.12336*, 2019.
- C. Ma, K. Wang, Y. Chi, and Y. Chen. Implicit regularization in nonconvex statistical estimation: Gradient descent converges linearly for phase retrieval and matrix completion. In *PMLR*, volume 80, pages 3345–3354, 10–15 Jul 2018.
- D. Martinec and T. Pajdla. Robust rotation and translation estimation in multiview reconstruction. In *2007 IEEE Conference on Computer Vision and Pattern Recognition*, pages 1–8. IEEE, 2007.
- T. Maunu and G. Lerman. Robust subspace recovery with adversarial outliers. *arXiv preprint arXiv:1904.03275*, 2019.
- T. Maunu, T. Zhang, and G. Lerman. A well-tempered landscape for non-convex robust subspace recovery. *Journal of Machine Learning Research*, 20(37):1–59, 2019.
- S. Mei, Y. Bai, and A. Montanari. The landscape of empirical risk for nonconvex losses. *The Annals of Statistics*, 46(6A):2747–2774, 2018.
- R. R. Meyer. Sufficient conditions for the convergence of monotonic mathematical programming algorithms. *J. Comput. System Sci.*, 12:108–121, 1976.
- I. Mizera. On depth and deep points: a calculus. *The Annals of Statistics*, 30(6):1681–1736, 2002.
- M. Moakher. Means and averaging in the group of rotations. *SIAM journal on matrix analysis and applications*, 24(1):1–16, 2002.
- Praneeth Netrapalli, UN Niranjan, Sujay Sanghavi, Animashree Anandkumar, and Prateek Jain. Non-convex robust pca. In *Advances in Neural Information Processing Systems*, pages 1107–1115, 2014.
- O. Ozyesil, A. Singer, and R. Basri. Stable camera motion estimation using convex programming. *SIAM Journal on Imaging Sciences*, 8(2):1220–1262, 2015.
- O. Özyeşil, V. Voroninski, R. Basri, and A. Singer. A survey of structure from motion*. *Acta Numerica*, 26:305–364, 2017.
- A. Perry, A. S. Wein, A. S. Bandeira, and A. Moitra. Message-passing algorithms for synchronization problems over compact groups. *Communications on Pure and Applied Mathematics*, 71(11):2275–2322, 2018.
- P. Petersen. *Riemannian geometry*, volume 171. Springer, 3rd edition, 2016.
- Q. Qu, Y. Zhang, Y. Eldar, and J. Wright. Convolutional phase retrieval via gradient descent. *IEEE Transactions on Information Theory*, 66(3):1785–1821, 2019.
- Q. Qu, Z. Zhu, X. Li, M. Tsakiris, J. Wright, and R. Vidal. Finding the sparsest vectors in a subspace: Theory, algorithms, and applications. *arXiv preprint arXiv:2001.06970*, 2020.
- R. Rado. A theorem on general measure. *Journal of the London Mathematical Society*, 1(4):291–300, 1946.
- D. M. Rosen, L. Carlone, A. S. Bandeira, and J. J. Leonard. SE-sync: A certifiably correct algorithm for synchronization over the special euclidean group. *The International Journal of Robotics Research*, 38(2-3):95–125, 2019.
- A. Singer. Angular synchronization by eigenvectors and semidefinite programming. *Applied and computational harmonic analysis*, 30(1):20–36, 2011.
- J. Sun, Q. Qu, and J. Wright. Complete dictionary recovery over the sphere. In *Sampling Theory and Applications (SampTA), 2015 International Conference on*, pages 407–410, May 2015a. doi: 10.1109/SAMP TA.2015.7148922.
- J. Sun, Q. Qu, and J. Wright. When are nonconvex problems not scary? *arXiv preprint arXiv:1510.06096*, 2015b.
- C. J. Taylor and D. J. Kriegman. Minimization on the Lie group $SO(3)$ and related manifolds. *Yale University*, 16:155, 1994.

- C. D. Toth, J. O'Rourke, and J. E. Goodman. *Handbook of discrete and computational geometry*. Chapman and Hall/CRC, 2017.
- R. Tron and R. Vidal. Distributed image-based 3-d localization of camera sensor networks. In *Decision and Control, 2009 held jointly with the 2009 28th Chinese Control Conference. CDC/CCC 2009. Proceedings of the 48th IEEE Conference on*, pages 901–908. IEEE, 2009.
- R. Tron, X. Zhou, and K. Daniilidis. A survey on rotation optimization in structure from motion. In *Proceedings of the IEEE Conference on Computer Vision and Pattern Recognition Workshops*, pages 77–85, 2016.
- J. W. Tukey. T6: Order statistics, in mimeographed notes for statistics 411. *Department of Statistics, Princeton University*, 1974.
- I. Waldspurger and A. Waters. Rank optimality for the Burer-Monteiro factorization. *arXiv preprint arXiv:1812.03046*, 2018.
- L. Wang and A. Singer. Exact and stable recovery of rotations for robust synchronization. *Information and Inference*, 2013.
- L. Wang and A. Singer. Exact and stable recovery of rotations for robust synchronization. *Information and Inference*, 2013. doi: 10.1093/imaiai/iat005.
- X. Yi, D. Park, Y. Chen, and C. Caramanis. Fast algorithms for robust PCA via gradient descent. In *NIPS*, pages 4152–4160, 2016.
- W. I. Zangwill. *Nonlinear Programming: A Unified Approach*. Engle-wood Cliffs, NJ: Prentice-Hall, 1969.
- T. Zhang and Y. Yang. Robust PCA by manifold optimization. *Journal of Machine Learning Research*, 19(80):1–39, 2018.
- Y. Zhang, Q. Qu, and J. Wright. From symmetry to geometry: Tractable nonconvex problems. *arXiv preprint arXiv:2007.06753*, 2020.